

Research Paper

Effects of Hole-Perpendicularity Error on Joint Stiffness of Single-Lap Double-Bolt Composite Joints

Xueshu LIU¹⁾, Yuxing YANG²⁾, Hang GAO²⁾, Yongjie BAO²⁾,
Rupeng LI³⁾, Lei CHEN³⁾

¹⁾ *School of Automotive Engineering*
Dalian University of Technology
Dalian 116024, P.R. China
e-mail: liuxs@dlut.edu.cn

²⁾ *School of Mechanical Engineering*
Dalian University of Technology
Dalian 116024, P.R. China

³⁾ *Shanghai Aircraft Manufacturing Co. Ltd.*
Shanghai 200120, P.R. China

To investigate the influence of hole-perpendicularity error on stiffness of single-lap double-bolt composite joints, a finite element model was first created and validated by using the analogical mass-spring based model proposed by MCCARTHY *et al.* The model was then modified by introducing hole-perpendicularity error, with which the influences of hole-perpendicularity error, which is represented by hole-tilting angle, hole-tilting direction, and bolt torque on the joint stiffness are studied. It is found that the hole-tilting direction causes the joint stiffness to either increase or decrease, which depends on the relation between the hole-tilting direction and the loading orientation. In addition, the hole-tilting angle strengthens the influence of hole-tilting direction and the bolt torque plays the most important role among the three factors in affecting the joint stiffness.

Key words: bolted joints, joint stiffness, hole-perpendicularity error, bolt torque.

1. INTRODUCTION

Carbon fiber reinforced plastic (CFRP) has been widely used in primary aircraft structures in recent years. Although the bolted joints are of lower structural efficiency when compared to adhesively bonded joints, they are still the major method of assembling structural elements in the aerospace industry largely due

to its facility to assemble, disassemble, and repair, as well as its tolerance to environmental effects [1]. Unfortunately, the joints are often the weakest parts of a structure, where damage often generates and evolves to cause final failure. The increased stress-intensity factor at the surrounding of the bolt hole makes the design and assembly process more critical in contrast to metallic components [2]. In addition, the weight of the aircraft may significantly increase due to the use of large number of bolted joints. It is essential to optimize the joint design for the sake of weight saving. Therefore, the study of mechanical joints in structural composite components has received considerable attention [3]. A review of the performance of bolted joints in composite materials is presented in [4].

Numerous reports have been presented on the mechanical response of composite joints, all of which can be classified into three groups: experiment based investigation [5–8], simulation based study [9–14] and analogical model based research [15–22]. Only analytical models shall be discussed here, as this is the configuration of interest in this work.

Mass-spring model had been used to predict joint stiffness and load distribution in composite joints for several decades. Recently, MCCARTHY *et al.* have developed this model to study the effect of bolt-hole clearance, friction coefficient, and torque level on multi-bolt composite joints [15]. The through-thickness stiffness in tension-loaded composite bolted joints was investigated by a variant in [19]. The mass-spring models have been applied preferentially to composite bolted joints while considering the equivalent stiffness of the composite plate. “The McCarthy model was modified to include the consideration of different spring elements to reproduce the stiffness of plies with different orientation. The bearing loads and displacements determined in the mass-spring model were used to evaluate the bearing failure of each ply. When the failure of any ply was verified, the corresponding spring element was removed from the mass-spring model to reproduce the damage” [20]. An accurate prediction of the load displacement response of single- and multi-fastener joints to complete failure can be done in a matter of seconds. TAHERI-BEHROOZ *et al.* investigated the effect of material nonlinearity on the load distribution in multi-bolt composite joints [21]. They combined the traditional spring-mass model with a nonlinear Tsai-Hahn formula to construct a new computational tool for joint design. It was found that increasing the degree of material nonlinearity of the members increased the amount of load transferred by the outer bolts of joint, while it decreased that of inner bolts. Moreover, mass-spring system was extended to hybrid composite joints. For example, ANDRIAMAMPINANINA *et al.* proposed a simple analytical method to describe the behavior of a hybrid load transfer bolted joint assembly [18]. BODJONA *et al.* proposed a model to study the load sharing in bonded/bolted composite joints [23]. Their model was confirmed both by experiment and a finite element model. All the above mentioned studies

prove that the mass-spring model can be used to predict the joint stiffness of composite joints.

Geometrical imperfections often occur during not only the manufacturing process of composite component like geometrical deviation but also in an assembly process such as hole-location error, which consequently affect the mechanical performance of composite structure. Many researchers focused on the problem occurring in manufacturing process like [24–26], while only in recent years geometrical imperfections taking place in assembly process have attracted the researchers' special interest. For example, LECOMTE *et al.* adopted mass-spring model to investigate the effect of hole-location error on load distribution in multi-bolted composite joints [27]. It has to be noted here that the influences of geometrical variation are always studied in the design process by using, for example, Monte Carlo-based method [28–30]. This method was only recently used for analyzing the influence of fiber orientation and thickness on geometrical variation outcome, and for predicting the stress levels for unidirectional composites during assembly [31]. When the anisotropic properties of composite material are taken into consideration, the traditional finite element method seems to be a good choice as it is shown in [32–34].

In this paper, the effects of hole-perpendicularity error on joint stiffness of single-lap double-bolt composite joints were investigated. The hole-tilting angle, hole-tilting direction and preload of fastener were studied. This paper is organized as follows. The construction and validation of the finite element model of single-lap double-bolt composite joints are given in details in the second section. The parameters of the studies joints are shown in the third section followed by the results and discussion presented in the fourth section. Conclusions are drawn in the last section.

2. MODELING OF SINGLE-LAP DOUBLE-BOLT COMPOSITE JOINTS

The model of single-lap double-bolt composite, used in this study, joint is shown in Fig. 1. Both the laminates are fabricated using a carbon fiber/epoxy composite material and protruding head joints are adopted. Laminates have a quasi-isotropic lay-up with stacking sequence $[45/0/-45/90]_{5s}$. Each ply has a nominal thickness of 0.13 mm and 5.2 mm, for each laminate. Geometrical parameters of the joints are listed in Table 1.

Table 1. Geometrical parameters of joints [mm].

t	l	p	e	w	ϕ_1	ϕ_2
5.2	40	36	24	48	8	15

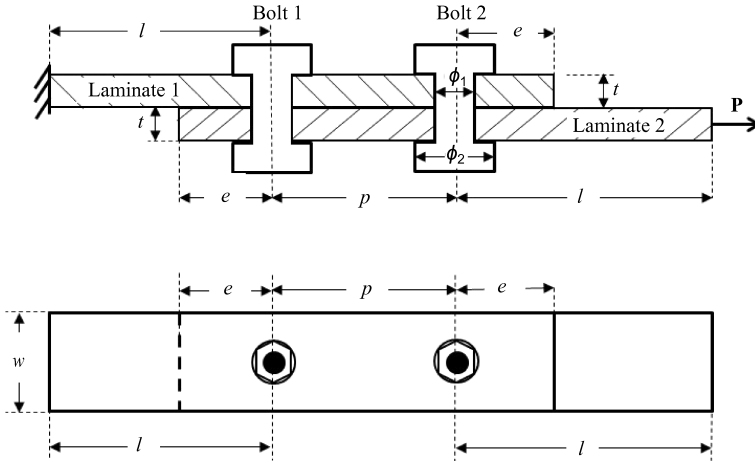


FIG. 1. Geometry and mass-spring model of a single-lap double-bolt composite joints.

The laminates are generally modelled in two ways. One approach involves the laminates to be modeled layer by layer, so that the stresses in each layer can be obtained, and this approach is usually used for the application of failure criteria to determine material strength [35–38]. The other method is to model laminates with homogeneous, orthotropic material properties, which is done for the sake of reducing computational complexity [15, 27, 39]. In this study, the second method was adopted as the macro-performance of joint is our concern and the elastic parameters are listed in Table 2. Note that, $E_{yy} = E_{xx}$, $G_{yz} = G_{xz}$ and $\nu_{yz} = \nu_{xz}$ are not listed in Table 2. The bolt is made from Titanium alloy and it is 8 mm in shank diameter and 15 mm for its head. Its properties are also given in Table 2.

Table 2. Material properties [39].

Homogenised laminate	E_{xx} [GPa]	E_{zz} [GPa]	G_{xy} [GPa]	G_{xz} [GPa]	ν_{xy}	ν_{xz}
	54.25	12.59	20.72	4.55	0.309	0.332
Titanium	E_b [GPa]	G_b [GPa]	ν			
	110	44	0.29			

2.1. Finite element modeling

With the geometrical parameters shown in Table 1, the finite element (FE) model (Fig. 2) was created using eight-node brick elements with incompatible modes, C3D8I in Abaqus. In this study, the bolt, the washer and the nut are considered to be one solid piece for the sake of simplicity and to avoid convergence problem as well.

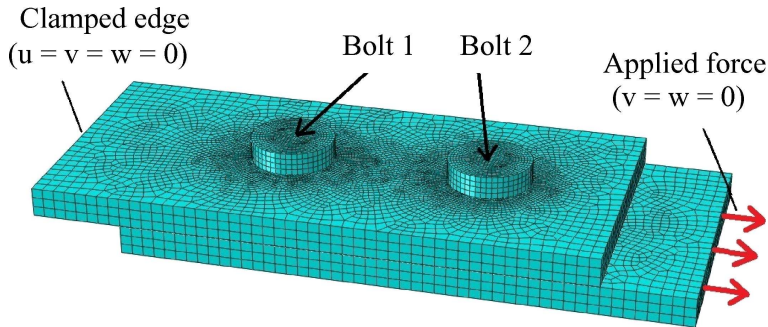


FIG. 2. The FE model of double-bolt composite joints.

The contact between the surfaces in the joint is modeled using the general contact algorithm. All neighboring surfaces are considered to come into a contact during the analysis including (i) between the laminates, (ii) between bolts (shanks and heads) and the holes, and (iii) between the nuts and the laminates. Finite sliding with a surface-to-surface option is applied to all possible contacts and the penalty approach is used to enforce the contact constraints, and a Coulomb friction is assigned to all surfaces with a friction coefficient of 0.42 [15].

As shown in Fig. 2, the free end of the top laminate is clamped. To apply the force on the free end of the bottom laminate, the motion of the surface was first constrained to a reference point chosen from the surface by using the coupling constraint available in Abaqus and the concentrated force was then applied to the reference point, which is not shown in Fig. 2.

In addition, mesh refinement is performed to get rid of an influence of mesh size on the simulation result. Considering the computation cost and accuracy, seeds with 2 mm distance for edges in black, 0.5 mm for red and 1 mm for green are assigned (Fig. 3) and the total number of meshes is almost 51k (Fig. 2). It takes nearly 2.4 hours to complete one computation on a computer with i7 CPU and 32G memory.

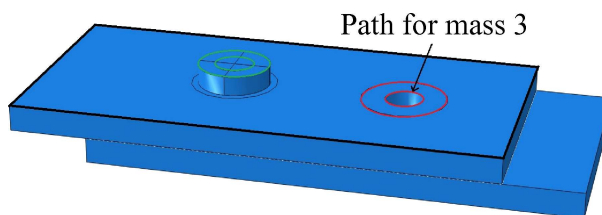


FIG. 3. Meshing strategy.

2.2. Model validation

The FE model was validated using the analytical model proposed by MCCARTHY and GRAY, in which the bolted joints were considered as a simple mass-spring system [15]. This approach has been proved and used by many researchers including [20, 40, 41]. The mass-spring system corresponding to the one shown in Fig. 1 is shown in Fig. 4. The stiffness of the region designated “Laminate 1” is marked by K_e and K_c , which indicate the spring stiffness between mass 1 and the free end, and masses 1 and 3, respectively. A similar convention is used for the bottom laminate. The bolt stiffness is represented by K_b . The joint load F is applied at mass 5.

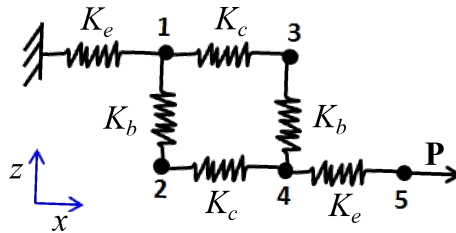


FIG. 4. Mass-spring system of single-lap double-bolt joints.

In the mass-spring system, the masses are free to move only in x direction and the springs have stiffness only in x direction too [40]. Based on these assumptions and under a quasi-static loading, the stiffness equation for this system is given as

$$(2.1) \quad [\mathbf{K}]\{\mathbf{X}\} = \{\mathbf{F}\}.$$

Substituting the stiffness of each spring element into Eq. (1), the expression of the mass-spring model for single-lap double-bolt composite joints is written as

$$(2.2) \quad \begin{bmatrix} K_b+K_c+K_e & -K_b & -K_c & 0 & 0 \\ -K_b & K_b+K_c & 0 & -K_c & 0 \\ -K_c & 0 & K_b+K_c & -K_b & 0 \\ 0 & -K_c & -K_b & K_b+K_c+K_e & -K_e \\ 0 & 0 & 0 & -K_e & -K_e \end{bmatrix} \begin{bmatrix} x_1 \\ x_2 \\ x_3 \\ x_4 \\ x_5 \end{bmatrix} = \begin{bmatrix} 0 \\ 0 \\ 0 \\ 0 \\ P \end{bmatrix}.$$

In Eq. (2.2), K_e and K_c can be found by Eq. (2.3), and the parameters are given in Tables 1 and 2:

$$(2.3) \quad K_e = \frac{E_{xx} \cdot w \cdot t}{L - \phi_1/2}, \quad K_c = \frac{E_{xx} \cdot w \cdot t}{p - \phi_1}.$$

The bolt stiffness contains the bolt shear stiffness K_{sh} , the bolt bending stiffness K_{bn} and the bearing stiffness of laminate K_{br} , which is shown in Eq. (2.4)

$$(2.4) \quad K_b = \frac{1}{K_{sh}} + \left(\frac{1}{K_{bn}} + \frac{2}{K_{br}} \right) (1 + 3\beta).$$

The factor $[1 + 3\beta]$ represents the fraction of the bending moment induced by non-uniform contact stresses in the laminates and $\beta = 0.15$ is recommended for the protruding head bolts [40].

Each element can be calculated according to Eq. (2.5), where G_b , A_b and E_b refer to the shear modulus, crossing section area of the bolt and Young's modulus of the bolt, t is the thickness of the laminate, and E_{xx} and E_{yy} are the homogenized longitudinal and transverse modulus of the laminate given in Table 2.

$$(2.5) \quad K_{sh} = \frac{3G_b A_b}{4t}, \quad K_{bn} = \frac{E_b t}{4}, \quad K_{br} = t \sqrt{E_{xx} E_{yy}}.$$

As introduced in [42], a finger-tight type bolt-torque is $0.5 \text{ N} \cdot \text{m}$ and $16 \text{ N} \cdot \text{m}$ for the bolt-torque in-service type for the bolt with 8 mm diameter. This pre-stress was implemented using a bolt pre-tension section in the 3D FE model. Note that the normal compressive force F_b produced by the bolt torque is found by the following equation

$$(2.6) \quad F_b = \frac{\tau}{k \cdot \phi_1},$$

where τ is the bolt torque and $k = 0.2$ is the torque coefficient [20].

Given $P = 10 \text{ kN}$, the displacements of all masses are obtained by using Eq. (2.2), and are used as a benchmark to validate the FE model. Note that in Eq. (2.2) the effect of friction is not considered. So in the FE analysis the bolt-torque of $0.5 \text{ N} \cdot \text{m}$ is adopted to get rid of the influence of friction. The results of the completed simulation are given in Table 3, including the relative error for each mass.

Table 3. FE model validation.

Mass	1	2	3	4	5
Analytical results [mm]	0.0266	0.1444	0.0369	0.1495	0.1764
FE analysis [mm]	0.0279	0.1318	0.0370	0.1407	0.1680
Relative Error [%]	4.9	-8.7	0.3	-5.9	-4.8

It can be seen that the displacements of masses 2, 4 and 5 are smaller than that of analogical calculation, while masses 1 and 3 are greater. This is due to

the fact that in the FE model contact between laminates has been taken into consideration and the penalty approach is used to enforce the contact constraints. Even though the pre-stress applied on bolt is finger-tight type, it must affect the displacements of masses. Such an effect is ignored in the analogical model. In addition, the parameters used in this study are mainly from [40]. But G_b is not clearly reported and an alternative was used for this computation, which may introduce errors. Finally, in the FE model masses are not defined as clear as in the analogical model. Taking mass 3 as an example, the averaged displacement of all nodes on the “Path for Mass 3”(small red circle in Fig. 3) is used to represent the displacement of mass 3 in this study. Despite the many differences, the relative errors between the corresponding masses are all less than 9% and the relative error of mass 5 is less than 5%, which indicates that the FE model can be used to investigate the stiffness of the joints.

3. PARAMETRIC STUDY

During assembly bolt holes are often drilled from one side of joint components to the other. When a hole perpendicularity error occurs, the bolt hole may tilt along any direction in space. However, considering the potential influence of hole-tilting direction on joint stiffness, two extreme cases are considered in this study as shown in Fig. 5. To distinguish the difference between the two cases, the angle α between the positive load orientation (blue arrow) and the positive hole direction (red arrow in Fig. 5) is used, where the orientation from the matching surface to the free surface of a component indicates the positive hole direction. When $\alpha < 90^\circ$, we say the hole tilts along the load direction. Otherwise, it is against the load direction ($\alpha > 90^\circ$).

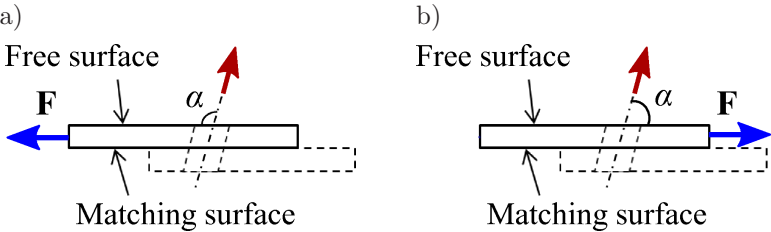


FIG. 5. Hole-tilting direction: the angle between the positive hole direction (red arrows) and the load direction (blue arrows): a) negative longitude, b) positive longitude.

After taking the symmetry of the joints into consideration, there are totally 5 joint types for single-lap, double-bolt composite joints as shown in Fig. 6, where red lines indicate the real hole axes, black lines represent the composite laminates, dashed blue lines signify the ideal axes of bolt holes and the black arrows are load orientations.

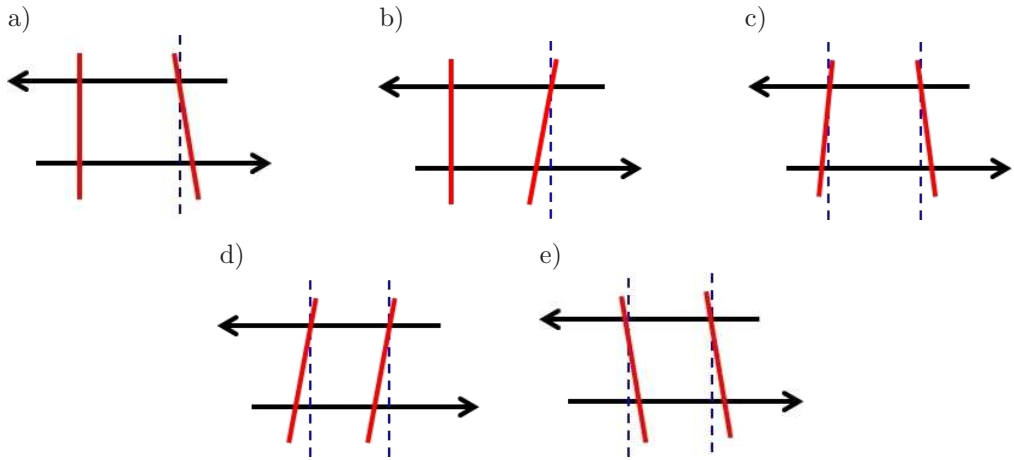


FIG. 6. The joint types of single-lap double-bolt composite joints with hole-perpendicularity error considered: a) T1, b) T2, c) T3, d) T4, e) T5.

Although hole-perpendicularity error is always used as an orientation control and defines how much the cylindrical surface of a hole may vary from being perpendicular to a specified datum, when t (in Fig. 1) is given the hole-perpendicularity error can be represented by the angle θ between the real axis of the hole OC' , and the ideal OC in the cross-section defined by OC' and OC (Fig. 7). In addition, bolt torques of different types are studied including the recommended in-service type and finger-tight type. The parameters to be investigated are shown in Table 4.

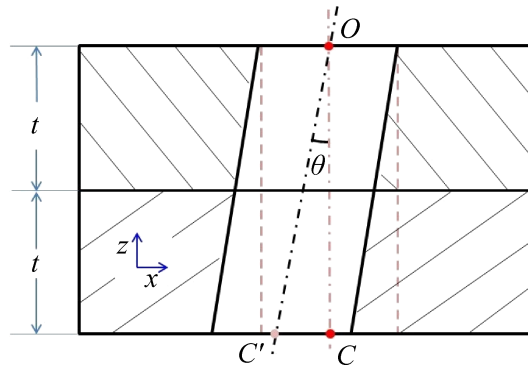


FIG. 7. Definition of hole-tilting angle: θ .

Table 4. Parameters.

Type of joint	T1, T2, T3, T4, T5
Perpendicularity error θ [°]	1, 2, 3, 4
Bolt torque τ [Nm]	$\tau_1 = 0.5$, $\tau_2 = 8$, $\tau_3 = 16$

Parametric study has been conducted to analyze the influences of hole-perpendicularity error, bolt torque and joint types on the stiffness of single-lap, double-bolt composite joints, and the results are shown in the following section.

4. RESULTS AND DISCUSSION

4.1. Effects of hole-tilting direction

The only difference between joint types T1 and T2, or T4 and T5 are the tilting directions of the bolt holes. So the influences of hole-tilting direction on joint stiffness can be obtained by analyzing the influences of joint types on joint stiffness. Simulation results are shown in Fig. 8, where the vertical axis shows the displacement of mass 5. Note that the bolt torques applied to both bolts are similar (τ_3) and for joint types T3, T4 and T5 the two bolt holes share the same hole-tilting angle but different tilting directions. It can be seen that among all the five joint types, T4 gains the maximum displacement of mass 5, followed sequentially by T2, T3, T1, and T5, no matter how much the hole-tilting angle is. In other words, T5 gets the maximum joint stiffness and the minimum for T4. Therefore, it can be concluded that the hole-tilting direction has a great effect on the joint stiffness. When the hole tilts in positive longitudinal direction ($\alpha < 90^\circ$), the joint stiffness is enhanced. Otherwise, it is weakened.

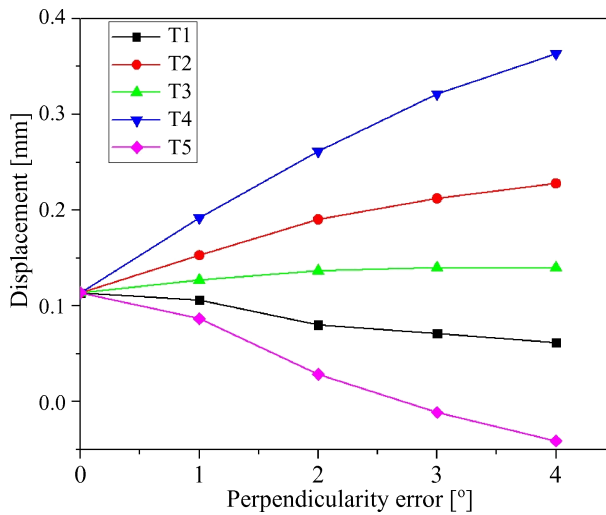


FIG. 8. The effect of joint type on joint stiffness.

The reason behind this phenomenon is that when the bolt is uploaded in the hole with perpendicularity error, one side of the hole wall is compressed due to the moment M caused by the load and the existence of hole-tilting angle, and as a result the assembly components have the trend to move in

opposite directions, which brings the variation of joint stiffness (Fig. 9). The influence of hole-perpendicularity error on joint stiffness for joint type T5 is illustrated in Fig. 10. When the holes are machined perfectly, the displacement Δ of the free end (mass 5 in Fig. 4) depends on the tensile load P . However, when hole-perpendicularity error exists, the loads applied to bolts may bring a displacement δ of the free end and this affects the macro-performance of the joint, which depends on the hole-tilting direction. For joint type T5, the final displacement of the free end is approximately $(\Delta - \delta)$, which means a higher joint stiffness. Once the hole-tilting direction varies, the joint stiffness will be lower. As for joint type T3, the joint stiffness is hardly affected because the holes tilt in opposite directions (green curve in Fig. 8).

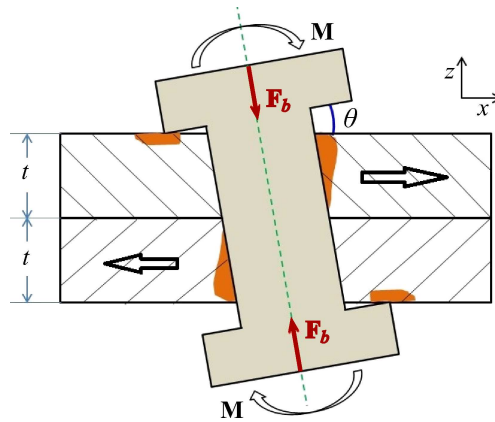


FIG. 9. Tendency to move and deform caused by hole perpendicularity error.

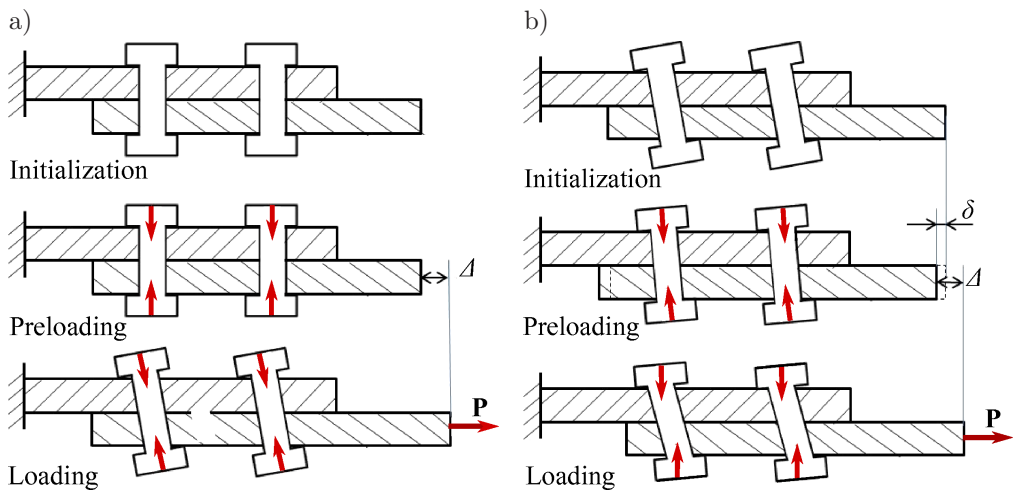


FIG. 10. Effect of hole-perpendicularity error on joint deformation: a) $\theta = 0$, b) $\theta \neq 0$.

4.2. Effect of hole-tilting angle

Generally speaking, the effect of θ on joint stiffness is to enhance the influence of hole-tilting direction. But the influence is first affected by joint type. In Fig. 8, it can be seen that for joint type T4 and T5, the influence of θ on joint stiffness is almost linear. But for T1 and T2, when $\theta > 2^\circ$ the influence can almost be disregarded. For T3, the influence can be ignored at all the time, due to the reason given above.

In addition, the influence of θ on joint stiffness is affected by tightening torques applied to joints. When the tightening torque is relatively high, the effect is obvious (Fig. 8). However, as shown in Fig. 11, when the tightening torque is finger-tight type, the influence of θ on joint stiffness can be disregarded.

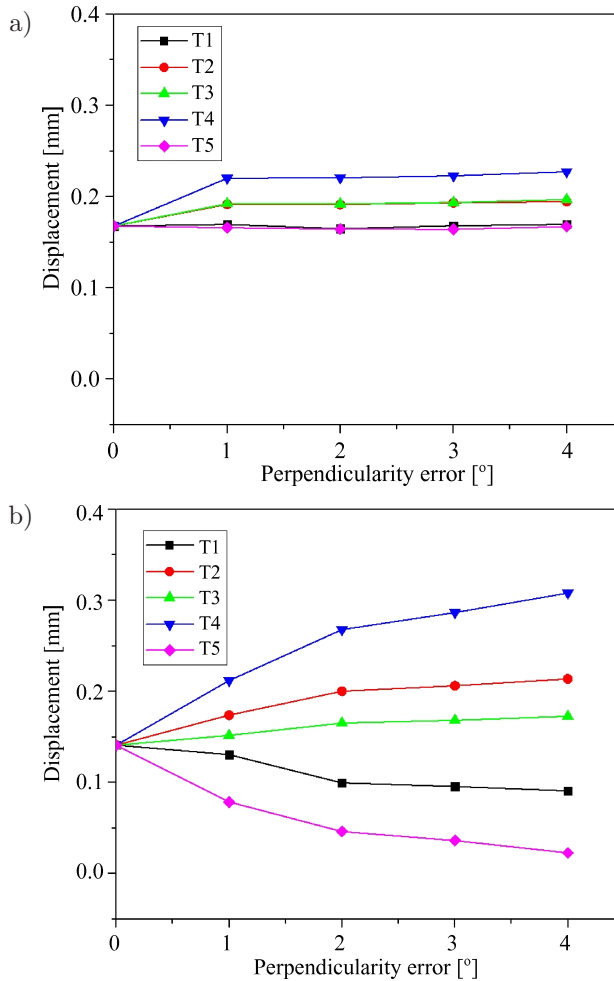


FIG. 11. Effect of tightening torque on the influence caused by θ : a) $\tau_1 - \tau_1$, b) $\tau_2 - \tau_2$.

4.3. Effect of bolt torque

It is well understood that the frictional force increases with increasing bolt torque and consequently the relative motion between assembly components is restrained, which results in increasing joint stiffness. When the holes are machined with hole-perpendicularity error, the situation changes. Taking joint type T5 as an example, due to the existence of hole-perpendicularity error, when the bolts are tightened the relative motion between assembly components occurs (Fig. 10), which can also be judged by the orientation of the frictional force. As given in Fig. 12 the legend ' $\tau_2 - \tau_2 - 1$ ' means the bolt torques applied to bolt 1 and 2 are both τ_2 and $\theta = 1^\circ$. It can be seen that when the bolt torque equals τ_3 and $\theta \geq 2$, the direction of frictional force keeps unchanged even after the tensile load is applied. This means that the joint stiffness is highly strengthened. Nevertheless, when the bolt torque equals τ_2 , the direction of frictional force alters. This indicates that for this joint type, the bolt torque has a greater effect on joint stiffness than that of hole-tilting angle.

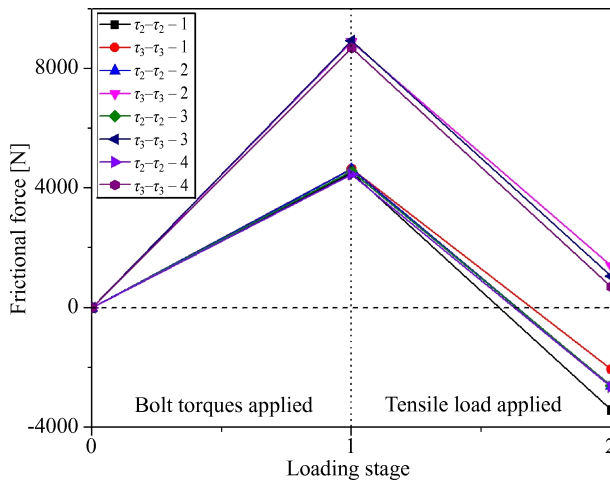


FIG. 12. Effect of hole perpendicularity error and bolt torques on frictional force.

The effect of bolt torque is affected by the joint type too. The influence of hole-tilting angle and bolt torque on joint stiffness of T2 is shown in Fig. 13. When the bolt torque is relatively low (τ_1), the increasing of hole-tilting angle has hardly any effect on the displacement of the joint's free end, namely, the joint stiffness. After the bolt torque increases up to τ_3 , the effect of θ becomes apparent, especially when $\theta > 2$. This indicates that the bolt torque has a deciding influence on joint stiffness.

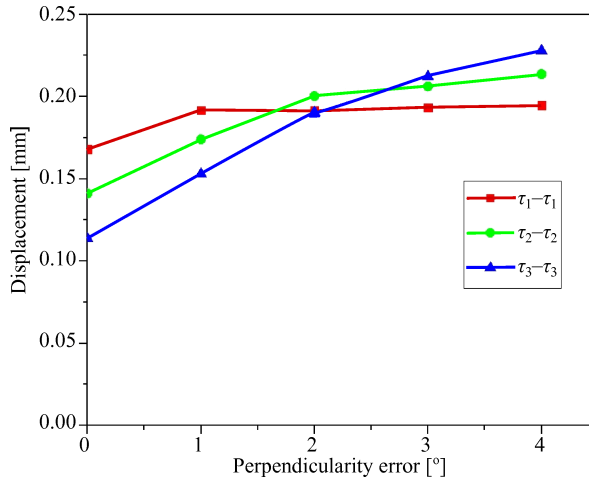


FIG. 13. Influence of hole-tilting angle and bolt torque on joint stiffness of T2.

5. CONCLUSION

In this paper, a parametric study was conducted by using the FE models to investigate the influences of hole-perpendicularity error on the joint stiffness of single-lap double-bolt composite joints. First, a model without hole-perpendicularity error was developed and validated by the analogical mass-spring model. After the hole-perpendicularity error was introduced into the FE model, the influences of hole-tilting angle, hole-tilting direction and bolt torque on the joint stiffness were studied. From the results shown in this paper, the following conclusions can be drawn

- The hole-tilting direction has a great effect on the joint stiffness. It may cause the increasing or decreasing of the joint stiffness, which depends on the relationship between the hole-tilting direction and the load orientation. However, this influence can be ignored when two adjacent holes tilt in opposite directions.
- The hole-tilting angle can only strengthen the effect of hole-tilting direction, but the influence is heavily affected by the bolt torques.
- The influence of bolt torque affects both the influences of hole-tilting direction and hole-tilting angle on joint stiffness and has the deciding effect on joint performance.

ACKNOWLEDGMENT

This work was supported by the Major State Basic Research Development Program [No. 2014CB046504], the National Natural Science Foundation of China

[grant number 51375068,51475073] and the Scientific Research Foundation for the Returned Overseas Chinese Scholars, State Education Ministry. The authors would like to acknowledge the above financial supports.

REFERENCES

1. CAMANHO P.P., MATTHEWS F.L., *A progressive damage model for mechanically fastened joints in composite laminates*, Journal of Composite Materials, **33**(24): 2248–2280, 1999.
2. SANTIUSTE C., OLMEDO A., SOLDANI X., MIGUELEZ M.H., *Delamination prediction in orthogonal machining of carbon long fiber-reinforced polymer composites*, Journal of Reinforced Plastics and Composites, **31**(13): 875–885, 2012.
3. CATALANOTTI G., CAMANHO P.P., *A semi-analytical method to predict net-tension failure of mechanically fastened joints in composite laminate*, Composites Science and Technology, **76**: 69–76, 2013.
4. COELHO A.M.G., MOTTRAM J.T., *A review of the behaviour and analysis of bolted connections and joints in pultruded fibre reinforced polymers*, Materials and Design, **74**: 86–107, 2015.
5. SUN H., CHANG F., QING X., *The response of composite joints with bolt-clamping loads. Part II: Model verification*, Journal of Composite Materials, **36**(1): 69–92, 2002.
6. STANLEY W.F., MCCARTHY M.A., LAWLOR V.P., *Measurement of load distribution in multi-bolt, composite joints, in the presence of varying clearance*, Journal of Plastics, Rubber and Composites, **31**(9): 412–418, 2002.
7. ZHAI Y., LI D., LI X., WANG L., YIN Y., *An experimental study on the effect of bolt-hole clearance and bolt torque on single-lap, countersunk composite joints*, Composite Structures, **127**: 411–419, 2015.
8. SALEEM M., ZITOUNE R., EL SAWI I., BOUGHERARA H., *Role of the surface quality on the mechanical behaviour of CFRP bolted composite joints*, International Journal of Fatigue, **80**: 246–256, 2015.
9. GRAY P.J., MCCARTHY C.T., *A global bolted joint model for finite element analysis of load distributions in multi-bolt composite joints*, Composites: Part B, **41**: 317–325, 2010.
10. GRAY P.J., MCCARTHY C.T., *A highly efficient user-defined finite element for load distribution analysis of large-scale bolted composite structures*, Composites Science and Technology, **71**: 1517–1527, 2011.
11. WANG Z., ZHOU S., ZHANG J., WU X., ZHOU L., *Progressive failure analysis of bolted single-lap composite joint based on extended finite element method*, Materials and Design, **37**: 582–588, 2012.
12. HUANG W., SUN Y., CHENG X., NIE H., *Tensile property of single countersunk bolt composite laminate joints*, Journal of Materials Engineering, **3**(12): 8–12, 2013.
13. ATAS A., SOUTIS C., *Strength prediction of bolted joints in CFRP composite laminates using cohesive zone elements*, Composites: Part B, **58**: 25–34, 2014.
14. LEONE F.A., DAVILA C.G., GIROLAMO D., *Progressive damage analysis as a design tool for composite bonded joints*, Composites: Part B, **77**: 474–483, 2015.

15. MCCARTHY C.T., GRAY P.J., *An analytical model for the prediction of load distribution in highly torqued multi-bolt composite joints*, *Composite Structures*, **93**: 287–298, 2011.
16. GANT F., ROUCH PH., LOUF F., CHAMPANEY L., *Definition and updating of simplified models of joint stiffness*, *International Journal of Solids and Structures*, **48**: 775–784, 2011.
17. LIU L., MAO Y., WEI R., *An analytical tool to predict load distribution of multi-bolt single-lap thick laminate joints*, [in:] 18th International Conference on Composite Materials, (ICCM) Jeju Island, Korea, 2011.
18. ANDRIAMAMPINANINA J., ALKATAN F., STEPHAN P., GUILLOT J., *Determining load distribution between the different rows of fasteners of a hybrid load transfer bolted joint assembly*, *Aerospace Science and Technology*, **23**: 312–320, 2012.
19. GRAY P.J., MCCARTHY C.T., *An analytical model for the prediction of through-thickness stiffness in tension-loaded composite bolted joints*, *Composite Structures*, **94**(8): 2450–2459, 2012.
20. OLMEDO A., SANTIUSTE C., BARBERO E., *An analytical model for predicting the stiffness and strength of pinned-joint composite laminates*, *Composites Science and Technology*, **90**: 67–73, 2014.
21. TAHERI-BEHROOZ F., SHAMAEI KASHANI A.R., HEFZABAD R.N., *Effects of material nonlinearity on load distribution in multi-bolt composite joints*, *Compositae Structures*, **125**: 195–201, 2015.
22. XIE Z.H., LI X., GUO J.P., XIONG X., DANG X., *Load distribution homogenization method of multi-bolt composite joint with consideration of bolt-hole clearance*, *Acta Materialiae Compositae Sinica*, **33**(4): 806–813, 2016.
23. BODJONA K., RAJU K., LIM G.H., LESSARD L., *Load sharing in single-lap bonded/bolted composite joints. Part I: Model development and validation*, *Composite Structures*, **129**: 268–275, 2015.
24. DAHLSTROM S., LINDKVIST L., *Variation simulation of sheet metal assemblies using the method of influence coefficients with contact modeling*, *Journal of Manufacturing Science and Engineering*, **129**: 615–622, 2006.
25. SAMPER S., ADRAGNA P.A., FAVRELIERE H., PILLET M., *Modeling of 2D and 3D assemblies taking into account form errors of plane surfaces*, *Journal of Computing and Information Science in Engineering*, **9**: 041005–1–12, 2009.
26. GANT F., ROUCH PH., CHAMPANEY L., *Updating of uncertain joint models using the Lack-of-Knowledge theory*, *Computers and Structures*, **128**: 128–135, 2013.
27. LECOMTE J., BOIS C., WARGNIER H., WAHL J.C., *An analytical model for the prediction of load distribution in multi-bolt composite joints including hole-location errors*, *Composite Structures*, **117**: 354–361, 2014.
28. WARMEFJORD K., LINDKVIST L., SODERBERG R., *Tolerance simulation of compliant sheet metal assemblies using automatic node-based contact detection*, [in:] Proceedings of IMECE2008 2008 ASME International Mechanical Engineering Congress and Exposition, Boston, Massachusetts, USA, 2008.
29. JARETEG C., WARMEFJORD K., SODERBERG R., LINDKVIST L., CROMVIK C., CARLSON J., EDELVIK F., *Variation simulation for composite parts and assemblies including variation in fiber orientation and thickness*, *Procedia CIRP*, **23**: 235–240, 2014.

30. SODERBERG R., WARMEFJORD K., LINDKVIST L., *Variation simulation of stress during assembly of composite parts*, CIRP Annals – Manufacturing Technology, **64**: 17–20, 2015.
31. BHAT M.R., VIJAYA KUMAR R.L., *Probabilistic stress variation studies on composite single lap joint using monte carlo simulation*, Composite Structures, **121**: 351–361, 2015.
32. TSAO C.C., *Effect of induced bending moment (IBM) on critical thrust force for delamination in step drilling of composites*, International Journal of Machine Tools & Manufacture, **59**: 1–5, 2012.
33. LIU L., ZHANG J., CHEN K., WANG H., *Influences of assembly parameters on the strength of bolted composite-metal joints under tensile loading*, Advanced Composite Materials, **22**(5): 339–359, 2013.
34. ZHOU Y., NEZHAD H.Y., HOU C., WAN X., MCCARTHY C.T., MCCARTHY M.A., *A three dimensional implicit finite element damage model and its application to single-lap multi-bolt composite joints with variable clearance*, Composite Structures, **131**: 1060–1072, 2015.
35. IRISARRI F.X., LAURIN F., CARRERE N., MAIRE J.F., *Progressive damage and failure of mechanically fastened joints in CFRP laminates. Part I: Refined finite element modelling of single-fastener joints*, Composite Structures, **94**: 2269–2277, 2012.
36. ZHANG J., LIU F., ZHAO L., CHEN Y., FEI B., *A progressive damage analysis based characteristic length method for multi-bolt composite joints*, Composite Structures, **108**: 2014.
37. SU Z.C., TAY T.E., RIDHA M., CHEN B.Y., *Progressive damage modeling of open-hole composite laminates under compression*, Composite Structures, **122**: 507–517, 2015.
38. DU D., HU Y., LI H., LIU C., TAO J., *Open-hole tensile progressive damage and failure prediction of carbon fiber-reinforced PEEK-titanium laminates*, Composites: Part B, **91**: 65–74, 2016.
39. MCCARTHY M.A., MCCARTHY C.T., LAWLOR V.P., STANLEY W.F., *Three-dimensional finite element analysis of single-bolt, single-lap composite bolted joint: part I – model development and validation*, Composite Structures, **71**: 140–158, 2005.
40. MCCARTHY M.A., MCCARTHY C.T., PADHI G.S., *A simple method for determining the effects of bolt-hole clearance on load distribution in single-column multi-bolt composite joints*, Composite Structures, **73**(1): 78–87, 2006.
41. WANG P., HE R., CHEN H., ZHU X., ZHAO Q., FANG D., *A novel predictive model for mechanical behavior of single-lap GFRP composite bolted joint under static and dynamic loading*, Composites: Part B, **79**: 322–330, 2015.
42. MCCARTHY C.T., MCCARTHY M.A., STANLEY W.F., LAWLOR V.P., *Experiences with modeling friction in composite bolted joints*, Journal of Composite Materials, **39**(21): 1881–1908, 2005.

Received June 2, 2016; accepted version August 30, 2016.
